Supplementary Information

Supplementary Table 1 | Data collection and refinement statistics (molecular replacement)

PDB ID	6M9T
Data collection	
Space group	C2
Cell dimensions	
a, *b*, *c* (Å)	120.80, 54.85, 96.80
α, β, γ (°)	90.0, 95.8, 90.0
Resolution (Å)	30.03-2.50 (2.62 – 2.50)[1]
R_{split} (%)	10. 5 (479.1)
CC*	0.9986 (0.569)
Completeness (%)	100 (100)
Redundancy	226.8 (88.2)[2]
Refinement	
Resolution (Å)	27.27 - 2.50
No. reflections / test set	22,101 / 1,050
R_{work} / R_{free}	0.200 / 0.242
No. atoms	
Protein	3,398
Ligands	26
Lipids and other	146
Wilson B (Å^2)	95.6
B-factors (Å^2)	
EP3	117.0
T4L	146.8
Ligand	92.7
Lipids and other	147.0
R.m.s. deviations	
Bond lengths (Å)	0.009
Bond angles (°)	0.95

[1]Highest-resolution shell is shown in parentheses.
[2]Data from 28,500 crystals

Supplementary Table 2 | Affinity of misoprostol-FA for EP3 receptor WT and mutants.

Domain	Mutant	pKi[1] (M)	SEM[1] (M)	p vs WT high[2,3]	p vs WT low[3]	n
	WT high	10.6	0.5	--	<0.0001	6
	WT low	7.7	0.1	<0.0001	--	
	EP3-T4L high	10.2	0.2	0.9999	<0.0001	4
	EP3-T4L low	7.69	0.03	<0.0001	>0.9999	
	Binding site position					
helix I	M58A	7.8	0.1	<0.0001	>0.9999	4
helix II	T106A	7.7	0.1	<0.0001	>0.9999	4
	T107A	8.37	0.06	<0.0001	0.9540	3
	V110A high	9.7	0.3	0.6009	<0.0001	3
	V110A low	8.0	0.1	<0.0001	>0.9999	
	Y114A	7.46	0.03	<0.0001	>0.9999	3
helix III	M137A	7.6	0.1	<0.0001	>0.9999	3
ECL2	T206A	8.17	0.05	<0.0001	0.9996	3
	T206V	8.32	0.04	<0.0001	0.9771	3
	W207A	7.8	0.2	<0.0001	>0.9999	3
	F209A	7.9	0.1	<0.0001	>0.9999	4
helix VI	L298A	7.86	0.03	<0.0001	>0.9999	3
helix VII	L329A high	10.3	0.4	>0.9999	<0.0001	3
	L329A low	8.08	0.09	<0.0001	>0.9999	
	V332A	7.88	0.01	<0.0001	>0.9999	3
	R333A	8.0	0.2	<0.0001	>0.9999	3
	R333L	8.05	0.04	<0.0001	>0.9999	3
	S336A	8.0	0.3	<0.0001	>0.9999	3
	Q339A	8.69	0.02	<0.0001	0.3702	3
	Others					
helix II	Q103A	7.75	0.01	<0.0001	>0.9999	3
	Q103L	7.67	0.05	<0.0001	>0.9999	3

[1]Value are the mean pKi ± SEM of indicated n independent experiments each done in triplicate.
[2]Significance was determined using one-way ANOVA analysis followed by a Tukey post-hoc statistical test against the high affinity and low affinity site for the WT receptor. $p < 0.0001$, F value is 15.54, among and within group degrees of freedom are 24 and 61, respectively.
[3]High and low refer to the high and low affinity binding, respectively.

Supplementary Table 3 | Agonist-induced signaling on EP3 receptor mutants.

Domain	Mutants	Misoprostol-FA			PGE_2		
		pEC_{50}[1] (M)	SEM[1] (M)	p vs WT[2]	pEC_{50}[1](M)	SEM[1] (M)	p vs WT[2]
	WT	8.97	0.02		9.62	0.04	
	Binding site						
helix I	M58A	8.69	0.08	0.3213	9.11	0.05	0.0156
helix II	T106A	8.65	0.08	0.1993	9.14	0.03	0.0242
	T106V	9.02	0.03	0.9995	9.6	0.1	0.9994
	T107A	9.1	0.1	0.9577	10.1	0.1	0.0146
	V110A	8.27	0.09	<0.0001	8.54	0.04	<0.0001
	Y114A	8.03	0.08	<0.0001	8.25	0.04	<0.0001
	Y114F	7.66	0.08	<0.0001	7.8	0.1	<0.0001
helix III	M137A	7.8	0.1	<0.0001	8.5	0.1	<0.0001
	G141A	9.08	0.03	0.9988	9.51	0.04	0.9988
	G141L	6.1	0.3	<0.0001	8.0	0.5	<0.0001
	G141W	6.7	0.1	<0.0001	6.3	0.2	<0.0001
ECL2	T206A	7.26	0.03	<0.0001	7.14	0.03	<0.0001
	T206V	7.54	0.06	<0.0001	7.38	0.01	<0.0001
	W207A	5.49	0.04	<0.0001	5.9	0.2	<0.0001
	F209A	6.93	0.03	<0.0001	7.33	0.03	<0.0001
helix VI	L298A	8.04	0.01	<0.0001	8.16	0.02	<0.0001
helix VII	L329A	6.87	0.02	<0.0001	6.90	0.02	<0.0001
	V332A	8.63	0.03	0.1368	8.69	0.06	<0.0001
	R333A	5.6	0.3	<0.0001	5.71	0.08	<0.0001
	R333L	7.06	0.03	<0.0001	7.26	0.08	<0.0001
	S336A	8.96	0.02	0.9998	9.68	0.07	0.9994
	Q339A	9.16	0.04	0.8663	9.75	0.09	0.9946
	Others						
helix I	A53F	8.87	0.04	0.9988	9.62	0.02	>0.9999
	F54A	8.47	0.06	0.0046	8.74	0.01	<0.0001
helix II	Q103A	8.4	0.1	0.0005	8.85	0.01	<0.0001
	Q103L	7.7	0.1	<0.0001	8.24	0.02	<0.0001
	G286A	8.97	0.05	>0.9999	9.76	0.05	0.9938
helix VII	I340A	7.43	0.02	<0.0001	7.49	0.04	<0.0001
	deltaC354[3]	8.88	0.06	0.9988	9.66	0.06	0.9997

[1]Value are the mean pEC_{50} ± SEM of 6 and 3 independent experiments for WT and all mutants, respectively.
[2]Significance for each compound was determined using one-way ANOVA analysis followed by a Dunnett post-hoc statistical test against mean EC_{50} determined for the WT receptor. For each compound $p < 0.0001$, and among and within group degrees of freedom are 29 and 63. F value are 104.7 and 114.1 for Misoprostol-FA and PGE_2, respectively.
[3]The deltaC534 is the WT receptor truncated at residue 354.

Supplementary Table 4 | Affinity of PGE_2 for EP3 receptor WT and mutants used to calculate misoprostol-FA pKi.

Domain	Mutant	pKi[1] (M)	SEM[1] (M)	n
	WT	8.72	0.09	4
	EP3-T4L	8.8	0.2	4
	Binding site			
helix I	M58A	8.2	0.3	4
helix II	T106A	8.1	0.1	4
	T107A	8.95	0.07	3
	V110A	9.1	0.3	3
	Y114A	8.06	0.09	3
helix III	M137A	7.9	0.1	3
ECL2	T206A	8.6	0.1	3
	T206V	8.71	0.06	3
	W207A	8.2	0.2	3
	F209A	8.4	0.2	4
helix VI	L298A	8.5	0.1	3
helix VII	L329A	8.9	0.1	3
	V332A	8.47	0.06	3
	R333A	8.48	0.07	3
	R333L	8.45	0.08	3
	S336A	8.7	0.2	3
	Q339A	9.0	0.2	3
	Others			
helix II	Q103A	8.35	0.07	3
	Q103L	8.2	0.2	3

[1]Value are the mean pKi ± SEM of indicated n independent experiments each done in triplicate.

Supplementary Table 5 | Sulprostone-Induced Signaling on EP3 Receptor Mutants.

Domain	Mutants	Sulprostone	
		pEC_{50}[1] (M)	SEM[1] (M)
	WT	9.7	0.1
helix II	Y114F	9.60	0.06
ECL2	T206A	8.67	0.06
	F209A	7.90	0.05
helix VI	L298A	8.66	0.04
helix VII	R333A	7.0	0.1

[1]Value are the mean pEC_{50} ± SEM of 3 independent experiments.

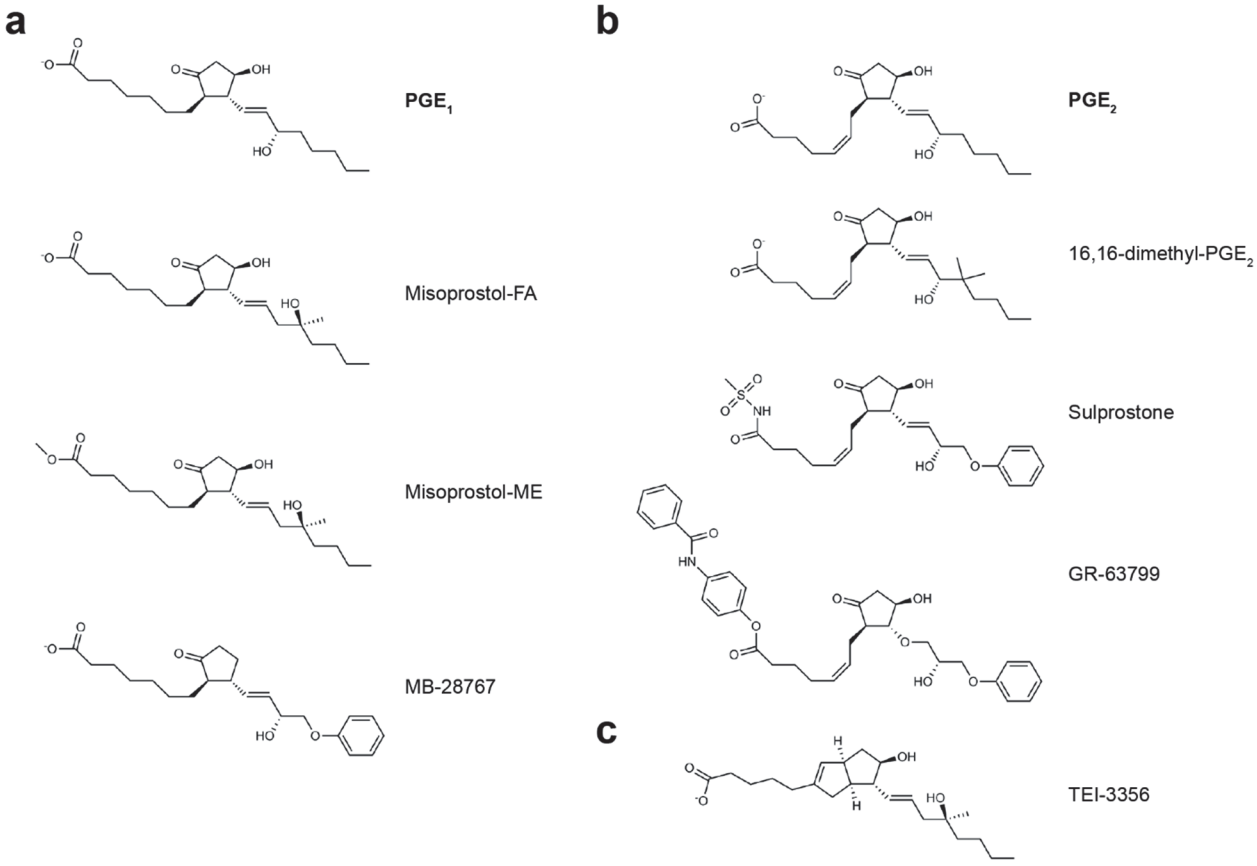

Supplementary Figure 1 | Comparison of 2-dimensional chemical structures of EP3 receptor agonists. Prostaglandin analogues of (**a**) PGE_1, (**b**) PGE_2 and (**c**) isocarbacyclin.

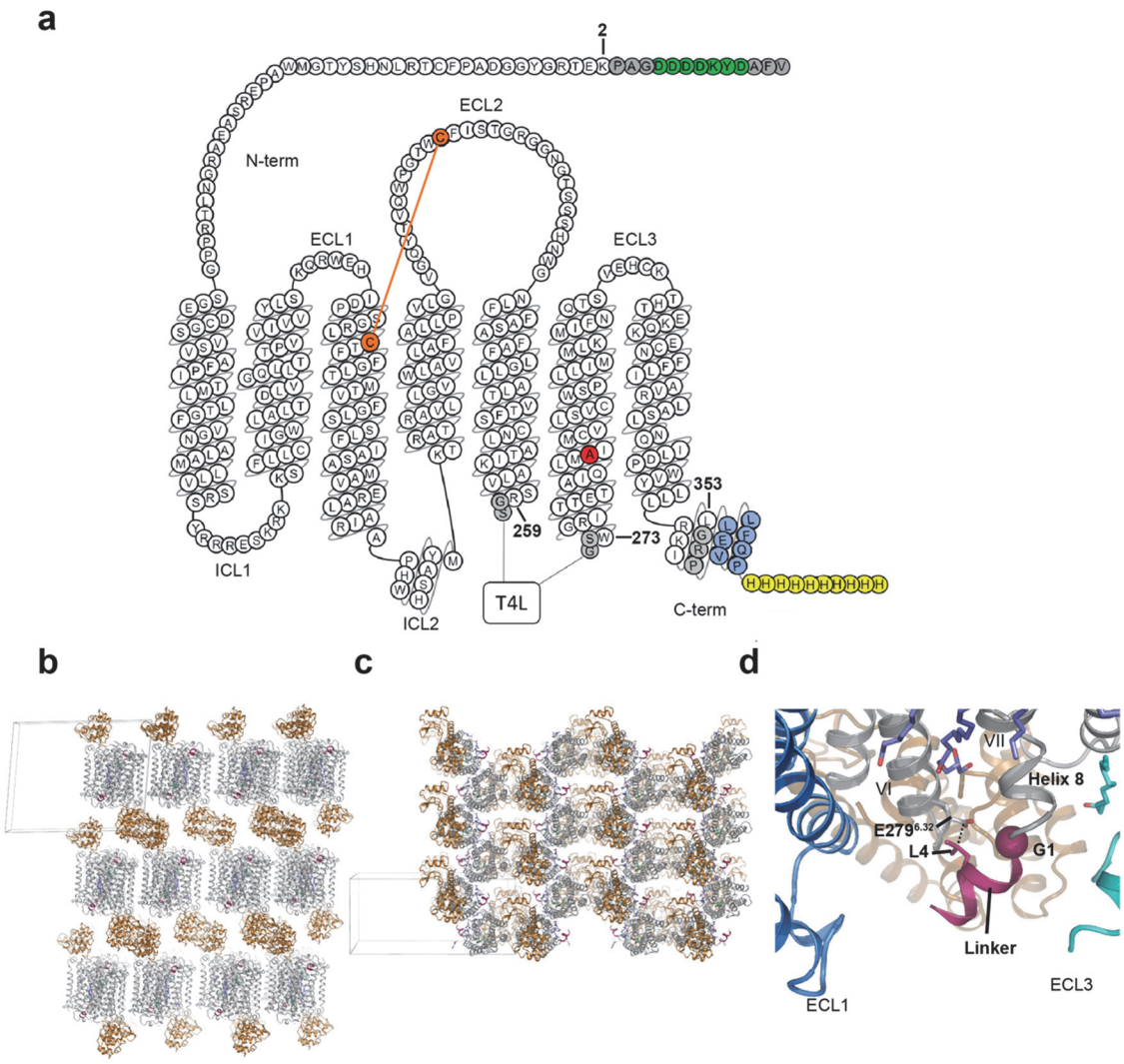

Supplementary Figure 2 | EP3-miso crystallization. (**a**) Two-dimensional representation of the amino acid sequence of the crystallization construct. Non-filled residues are native sequence of EP3 receptor. Gly286$^{6.39}$Ala is indicated as red-filled residue. Cys130$^{3.25}$ and Cys208 residues are orange-filled. Disulfide bond is indicated as orange line. Residues colored in gray, green, yellow, and blue are non-native linkers, FLAG and poly-histidine affinity tag sequences, and precision protease cleavage site, respectively. (**b**) Side view and (**c**) top view of EP3 receptor crystal packing in the monoclinic space group *C*2. (**d**) Close-up view of the precision protease cleavage site fused to the truncated C-terminus of EP3 receptor in the construct used for crystallization. Two

antiparallel and contiguous EP3 monomers in the crystal are shown as cyan and dark blue cartoon. The precision protease cleavage site sequence is shown in magenta as cartoon with the first residue (G1) shown as sphere. Lipids and indicated residues are shown as sticks. EP3 receptor is shown as gray cartoon. T4-lyzozyme is shown as gold cartoon. Dotted line represents a 3.5 Å non-polar contact.

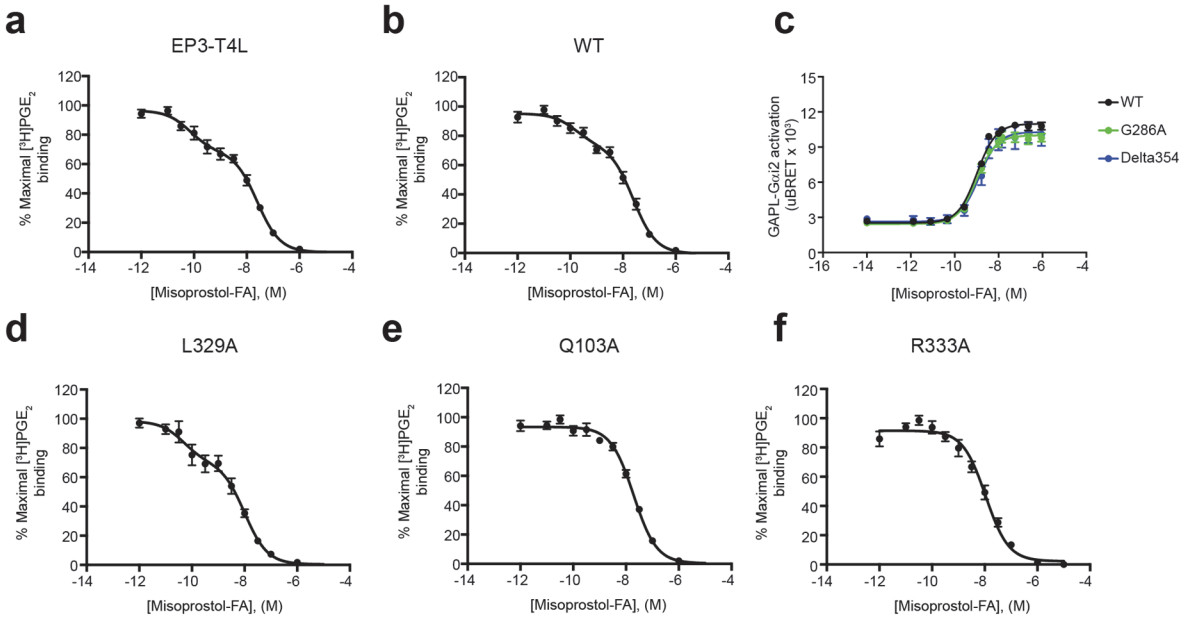

Supplementary Figure 3 | Pharmacology of misoprostol-FA on EP3 receptor. Competition binding assay of misoprostol-FA using [^{3}H]PGE$_2$ as a tracer on (**a**) EP3-T4L, (**b**) WT or (**d-f**) mutated EP3 receptors harbouring the indicated modification. (**c**) Misoprostol-FA-induced signaling on different EP3 receptor modifications. Each dot shows the mean ± SEM of 4, 6 and 3 independent experiments in triplicate for the EP3-T4L, WT and mutant binding data, respectively, and 3 independent experiments for the signaling data. Data were regressed as described in the methods. Corresponding pKi and pEC$_{50}$ are shown in the **Supplementary Tables 2-4**.

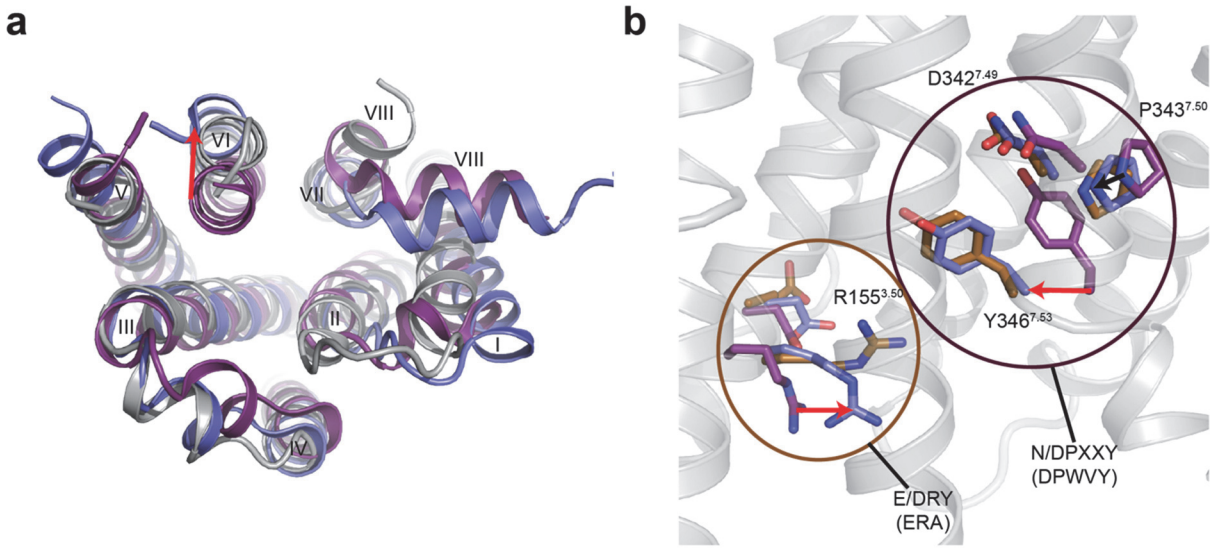

Supplementary Figure 4 |. Misoprostol-FA-induced active conformation of EP3 receptor. (**a**) Intracellular view of EP3 receptor. EP3 receptor, active Cannabinoid receptor 1 (Cb1) (PDB code 5xra), and inactive Cb1 (PDB code 5tgz) are shown as gray, blue, and maroon, respectively. (**b**) Side chains of E/DRY and N/DPxxY micro-switches of EP3 receptor, active Cb1 (PDB code 5xra), and inactive Cb1 (PDB code 5tgz) are shown in gold, blue, and maroon sticks, respectively. EP3 receptor main chain is shown as gray cartoon. The red arrows indicate an activating conformational change.

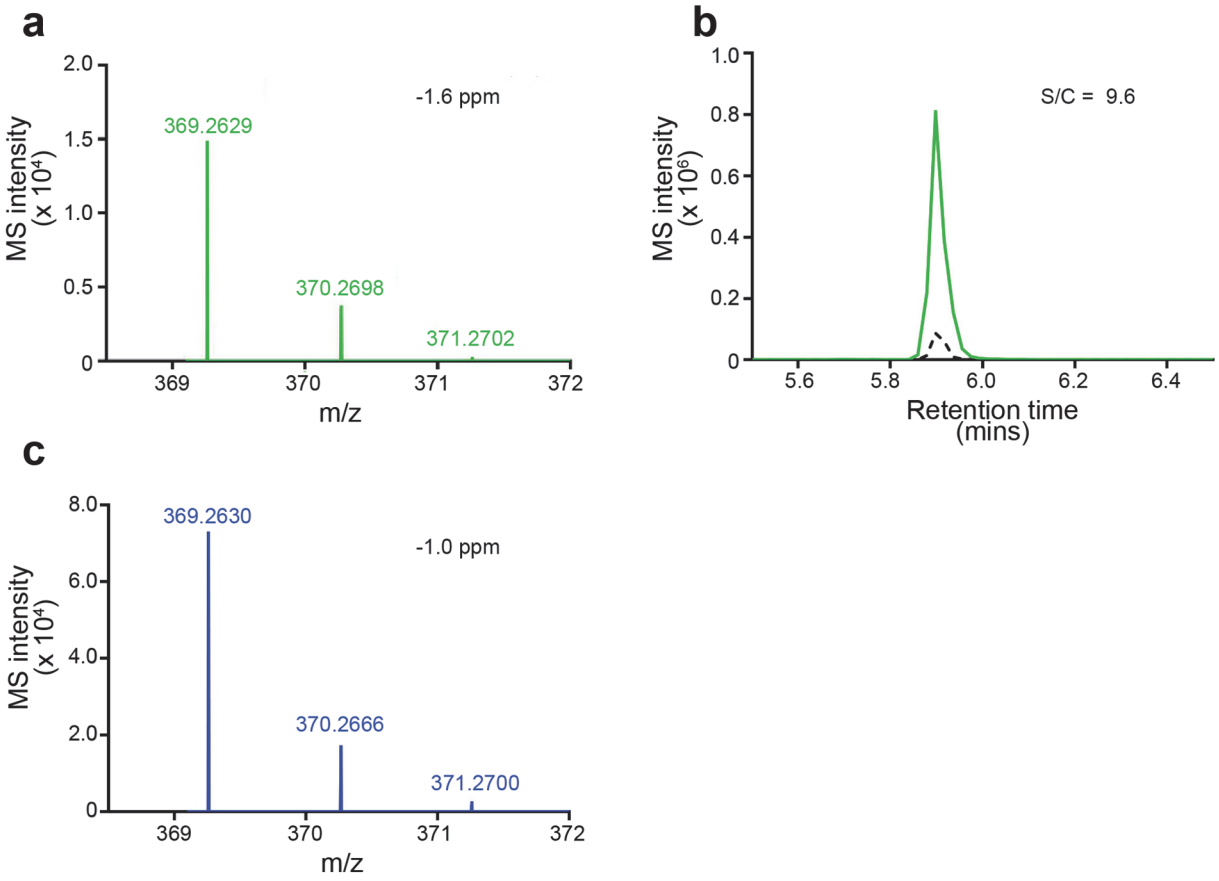

Supplementary Figure 5 | Binding of misoprostol-FA to purified EP3 receptor by mass spectrometry. (**a**) A representative high-resolution MS spectrum and (**b**) LC-MS chromatograms for misoprostol-FA detected in the purified EP3-T4L receptor. Extracted ion chromatograms of misoprostol-FA detected in the EP3 receptor sample and the human A_{2A} adenosine receptor control are indicated by a solid line and a dashed line, respectively. (**c**) The mass spectrum of misoprostol-FA from the compound standard. Mass error of the mono-isotope peak compared to the theoretical accurate mass of misoprostol-FA (369.2635 *m/z*) is indicated in each panel. The experiment was repeated 3 times independently with similar results.

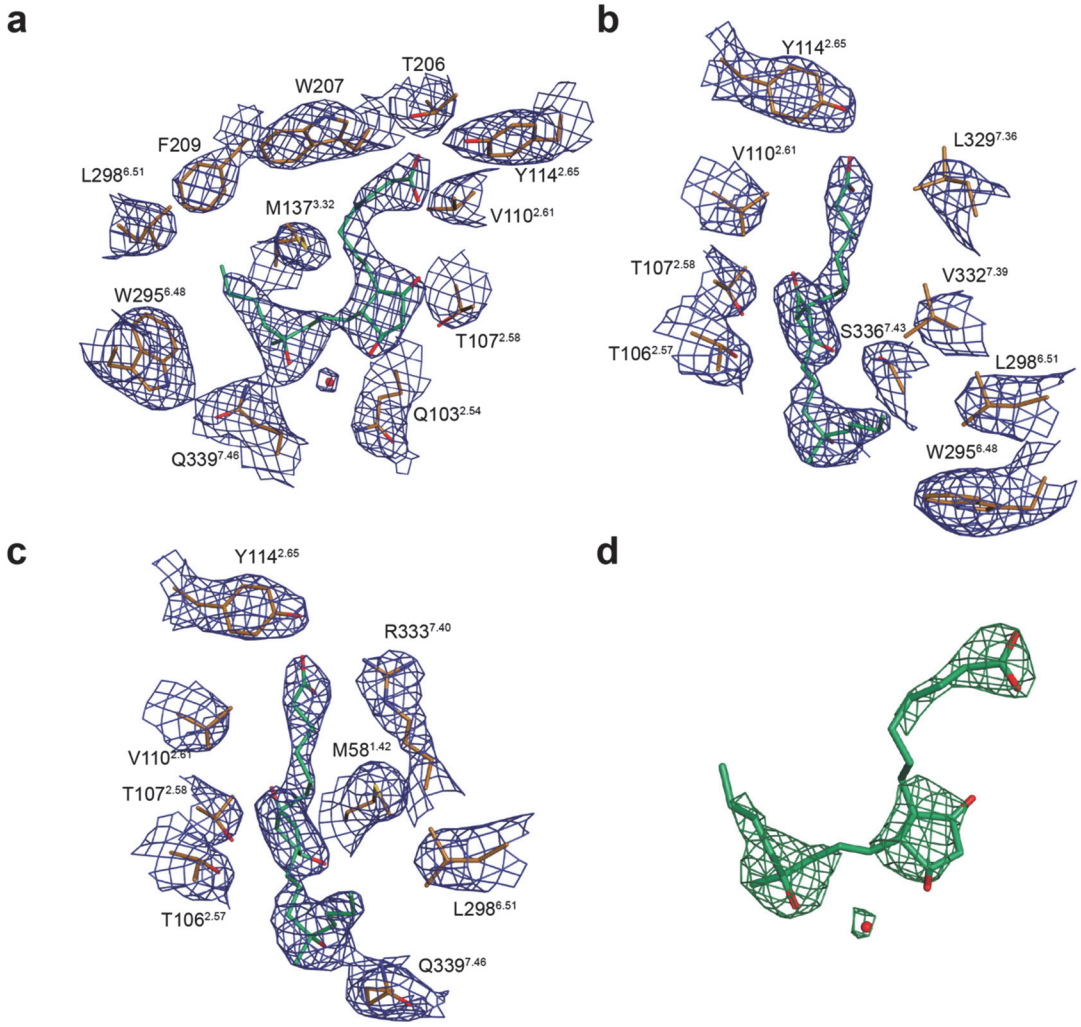

Supplementary Figure 6 | Electron density maps of EP3-miso structure. (**a-c**) 2Fo-Fc electron density maps of EP3-miso binding site contoured at 1 σ. (d) Simulated annealing ligand omit Fo-Fc electron density map for misoprostol-FA and the binding site water molecule contoured at 2.7 σ. Residues of the binding site and misoprostol-FA are shown in stick gold and green, respectively. Water molecule is shown as a red sphere.

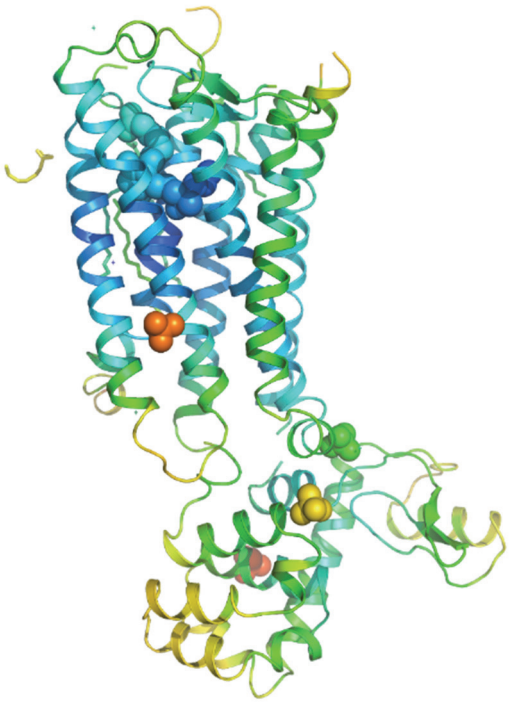

Supplementary Figure 7 | B-factor distribution on the EP3 crystal structure. EP3 receptor is shows as ribbons, lipids are shows as sticks, and misoprostol-FA and sulfate ions as spheres. Colors represent B-factor for Misoprostol-FA and lipid atoms, protein residues and sulfate ions ranging from dark blue (60 $Å^2$) to red (220 $Å^2$).

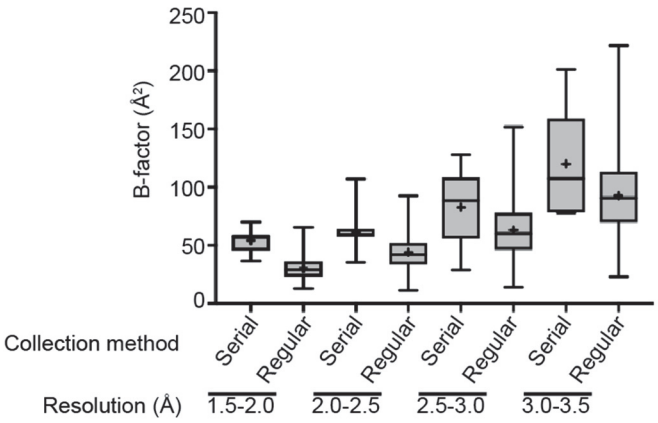

Supplementary Figure 8 | Comparison of the B-factors from membrane protein structures solved from data collected using serial crystallography vs traditional crystallography. B-factor data was downloaded, binned and plotted as box and whisker where boxes represent the 25th and 75th percentile, the center line is the median, whiskers are minimum and maximum values, plus sign indicate the mean. The data are from records at the Protein Data Bank for published membrane protein structures collected using serial crystallography (serial, 58 structures) and traditional synchrotron crystallography (regular, 1650 structures).